

Time Evolution of Collisionless Shock in Counterstreaming Laser-Produced Plasmas

Y. Kuramitsu,^{1,*} Y. Sakawa,¹ T. Morita,² C. D. Gregory,³ J. N. Waugh,⁴ S. Dono,⁵ H. Aoki,² H. Tanji,⁵ M. Koenig,³
N. Woolsey,⁴ and H. Takabe¹

¹*Institute of Laser Engineering, Osaka University, 2-6 Yamadaoka, Suita, Osaka, 565-0871 Japan*

²*Graduate School of Science, Osaka University, 1-1 Machikaneyama-cho, Toyonaka, Osaka 560-0043, Japan*

³*Laboratoire pour l'Utilisation des Lasers Intenses, UMR 7605, CNRS-CEA-Université Paris VI-Ecole Polytechnique, 91128 Palaiseau Cedex, France*

⁴*Department of Physics, University of York, York, YO10 5DD, United Kingdom*

⁵*Graduate School of Engineering, Osaka University, 2-1, Yamadaoka, Suita, Osaka 565-0871, Japan*

(Received 28 October 2009; published 26 April 2011)

We investigated the time evolution of a strong collisionless shock in counterstreaming plasmas produced using a high-power laser pulse. The counterstreaming plasmas were generated by irradiating a CH double-plane target with the laser. In self-emission streaked optical pyrometry data, steepening of the self-emission profile as the two-plasma interaction evolved indicated shock formation. The shock thickness was less than the mean free path of the counterstreaming ions. Two-dimensional snapshots of the self-emission and shadowgrams also showed very thin shock structures. The Mach numbers estimated from the flow velocity and the brightness temperatures are very high.

DOI: 10.1103/PhysRevLett.106.175002

PACS numbers: 52.35.Tc, 52.38.Mf, 52.72.+v

While in ordinary gas the minimum thickness of a shock front is at least of the order of the mean free path of the molecules, in collisionless plasmas the thickness of a shock front is considerably smaller than the mean free path as a result of cooperative phenomena [1]. There are two possibilities for collisionless shock formation in an unmagnetized plasma: one is an electrostatic shock, and the other is a Weibel-mediated shock. Electrostatic shocks with a relatively low Mach number and slow flow speed have been investigated in laboratory plasmas since the 1970s [2,3]. A recent paper has shown that the shock transition is due to enhanced Landau damping [4]. Recent theoretical and numerical study suggests that very-high-Mach-number electrostatic shocks can also form [5]. Two-dimensional particle-in-cell simulations show that a magnetic field self-generated via the Weibel instability deflects upstream plasma flow and acts as an effective dissipation mechanism, resulting in shock formation [6,7]. These two types of collisionless shock have not yet been seen in laboratory experiments and observations have not yet demonstrated their astrophysical existence. In order to clarify which process is dominant in nonrelativistic astrophysical shocks, where the plasma flow velocities are hundreds to thousands of km/s, fast plasma flows are necessary when carrying out an experiment, and current high-power laser facilities allow us to perform such experiments.

In this Letter we report the first experimental results for the time evolution of a strong collisionless shock in counterstreaming plasmas produced using a high-power laser system, Gekko XII (GXII). Irradiating CH double-plane targets with the laser pulse, we produced counterstreaming plasmas and observed them using streaked interferometry. In addition, using streaked optical pyrometry (SOP) increases in

the self-emission were observed as the two-plasma interaction evolved; two-dimensional images of the self-emission taken using a gated optical imager (GOI) clearly show a smooth shock structure. Shock transition layers, corresponding to sudden density changes, were observed using shadowgraphy at similar positions to the self-emission increases. The mean free paths of ions, estimated from the plasma density and the counterstreaming relative velocity, were larger than the shock transitions, tending to become smaller later in time. The compression ratio in this collisionless regime was larger than 4. The brightness temperatures of the plasmas yield very-high-Mach numbers. These results strongly indicate the formation of very-high-Mach-number electrostatic collisionless shocks in the laboratory plasmas, as predicted in [5].

The experiment was performed using the GXII laser system at the Institute of Laser Engineering, Osaka University. The laser conditions were wavelength 351 nm, pulse length 500 ps, focal spot diameter 300 μm , pulse energy ~ 100 J. Figure 1 shows a schematic drawing of the configuration of the laser and the double-plane target. Both planes were of 60 μm thickness and they were in parallel with a separation of 4.5 mm. The target normal was aligned 30° from the laser propagation axis in order to use the laser to irradiate the right-hand plane and produce ablation plasma on its front side. The left plane was ionized by radiation and scattered laser light coming from the right plane. The diagnostics were transverse to the axis of the plasma, with two streak cameras and three intensified charge coupled devices (ICCD). The details of the diagnostics are in [8]. The slits of the streak cameras were rotated in order to measure the time evolution of the plasmas along a line parallel to target normal.

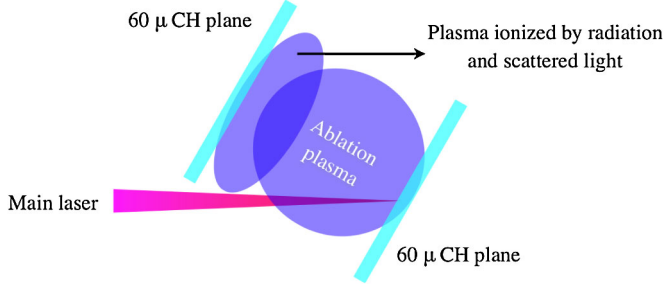


FIG. 1 (color online). Schematic of the double-plane target. The separation between two planes was 4.5 mm. The target normal lies 30° from the laser axis.

Figures 2(a) and 2(b) show a streaked interferogram and an SOP image take on the same shot. We have processed the data such that the time axis is horizontal; the dashed horizontal line in Fig. 2(a) indicates the main laser arrival timing, $t = 0$. In the images the vertical dashed lines represent the target position and the spatial and temporal scales are identical. The axes on the top and right sides show the same quantities as the axes on the bottom and left

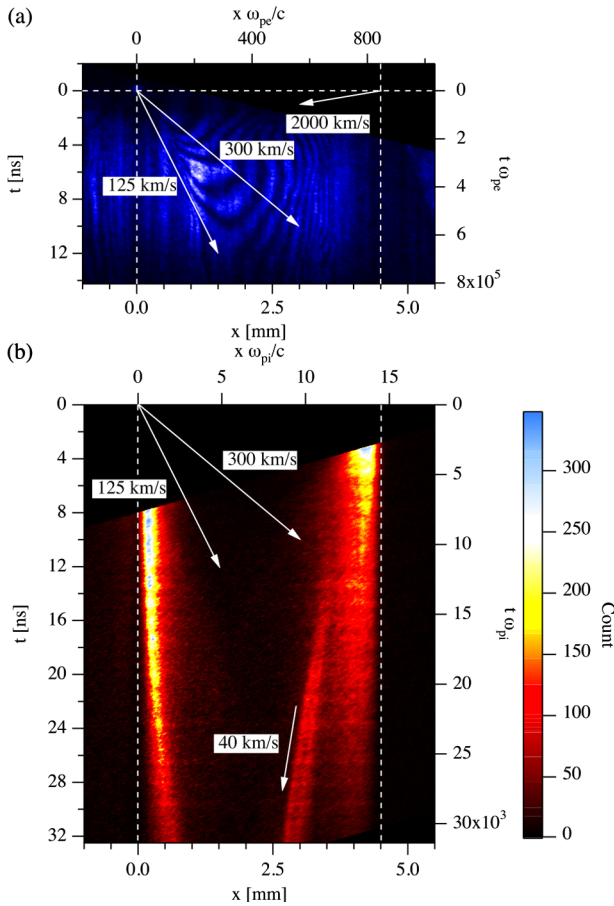


FIG. 2 (color online). (a) Streaked interferogram. The horizontal and vertical dashed lines represent the main laser timing and the target positions, respectively. (b) SOP image taken on the same shot as the interferogram in (a). The laser timing corresponds to the top of the image.

sides after normalization using the plasma frequencies with a reference value of the electron density $n_e = Zn_i = 10^{18} \text{ cm}^{-3}$, where Z is the charge number and n_i is the ion density. The streaked interferogram shows vertical fringes when there is no plasma; fringe shifts appear when there is a plasma. In Fig. 2(a), two fast, counterstreaming plasmas are seen. While there are no data for the right-hand plane at the main laser timing, where data are available a fringe shift is seen at $x = 1.5 \text{ mm}$ at $t = 1.5 \text{ ns}$, indicating that the velocity of the ablation plasma from the right plane was at least 2000 km/s. The plasma from the left plane with a density in the range measurable using our interferometer had a velocity of 125–300 km/s; the measurable density range was about 10^{18} – 10^{19} cm^{-3} , estimated from ICCD images of the plasma expansion taken at early times [8]. Note that after the plasmas expand in the whole ICCD image, it is difficult to obtain the density map from the interferogram; the density will decrease as the plasma expands. The fast plasmas are not visible in the SOP image in Fig. 2(b); at early times visible emission can only be seen near to the targets. A sharp structure appears once the plasma from the left plane reaches the plasma near to the right plane. The fact that the plasma from the left plane goes through the fast plasma from the right plane is evidence of the collisionless interaction of the fast counterstreaming plasmas. It is considered that the enhanced self-emission of the sharp structure results from an interaction between the fast plasma from the left plane and the plasma near to the right plane; the sharpness of the structure indicates that a shock wave was excited. This shock propagated from the right to the left at 40 km/s, and the trajectory is well described as $x = x_0 - V_s t$, where $x_0 = 3.92 \text{ mm}$ and the shock velocity $V_s = 40 \text{ km/s}$.

Temperature calibration of the SOP has been carried out [9]. The SOP counts for upstream and downstream plasma were typically 10 and 80–100, and the corresponding brightness temperatures are 0.78 and 1.7–1.9 eV, respectively. The sound velocity in the upstream of the shock is $c_1 \equiv (Zk_B T_e / m_i)^{1/2} \sim 6.3 \text{ km/s}$, where k_B is the Boltzmann constant, T_e is the electron temperature, and m_i is the ion mass, and we have considered that in the upstream the electron is isothermal in the wave scale and that the ion temperature is negligible. Since the probe laser went through the plasmas they are optically thin at the wavelength observed by the SOP, and consequently the brightness temperatures calculated using the SOP data underestimate the temperature, giving a minimum threshold. The downstream sound velocity, given by $c_2 \equiv [(Zk_B T_e + \gamma k_B T_i) / m_i]^{1/2}$, where γ is the ratio of the specific heats and T_i is the ion temperature, and we assume that in the downstream the ion is adiabatic ($\gamma = 5/3$) and $T_i = T_e$, must be larger than the downstream flow velocity in the shock frame. Assuming the downstream is at rest in the laboratory frame, the minimum downstream temperature is estimated as $T_2 = 21 \text{ eV}$ using $c_2 = v_2 = V_s$, where v_2 is the downstream flow velocity in the shock

frame. Assuming a gray body temperature, the upstream temperature is estimated as $T_1 \sim 3.1\text{--}3.7$ eV when $c_2 = v_2$, corresponding to $c_1 \sim 13\text{--}14$ km/s.

The mean free path of ions is written as $\lambda_{ii} = 2\pi\epsilon_0^2 m_i^2 \langle v_i \rangle^4 / (n_i Z^4 e^4 \ln\Lambda)$ [10], where ϵ_0 is the vacuum dielectric constant, $\langle v_i \rangle$ is the average ion velocity, Ze is the ion charge, $\ln\Lambda = \ln[\lambda_D 4\pi\epsilon_0 m_i \langle v_i \rangle^2 / (Z^2 e^2)]$, and λ_D is the Debye length. For the interaction between the fast plasmas the relative velocity of the counterstreaming ions is $2125 \text{ km/s} \leq \langle v_i \rangle \leq 2300 \text{ km/s}$ (the ion thermal velocity is negligible here). Using $Z = 3.5$ and a mass number $A = 6.5$, which are average values for a proton-carbon ion plasma, and also using $n_e = Zn_i = 10^{18} \text{ cm}^{-3}$, and $T_e = 21$ eV, the mean free path is estimated as $3.2 \text{ m} \leq \lambda_{ii} \leq 4.3 \text{ m}$. Since the mean free path is much larger than the system length of 4.5 mm, the counterstreaming interaction of fast plasmas is essentially collisionless.

Figure 3(a) shows a stack of line profiles taken from the SOP image in Fig. 2(b) at $7 + 2n$ ns, where n is an integer between 0 and 10. For ease of view, $20n$ counts have been added at each time. The top axis shows the spatial scale normalized to the ion inertial length. In Fig. 3(a), from 7 ns ($t\omega_{pi} = 6.8 \times 10^3$) to 9 ns ($t\omega_{pi} = 9.7 \times 10^3$) the profiles grow continuously from left to right as there is no interaction; the plasma from the right plane simply expands thermally. At 13 ns ($t\omega_{pi} = 1.3 \times 10^4$) one can see a structure formed at $x \sim 3.4$ mm ($x\omega_{pi}/c = 11$). As time evolves its profile steepens and it propagates to the left. The shock thickness was typically $100 \mu\text{m}$ ($x\omega_{pi}/c = 0.32$, $x\omega_{pe}/c = 18.8$, $x/\lambda_D = 3.1 \times 10^3$), thus, the electron dynamics must play an essential role in the shock formation. The ion-electron mean free path, estimated using a formula similar to that above, is $6.5\text{--}8.8 \times 10^{-7}$ m, where for the average velocity we have used the sum of the bulk velocity in the upstream and the electron thermal velocity in the downstream. This is much smaller than the shock thickness, however, since the ratio of plasma frequency to the electron-ion collision frequency $\omega_{pe}/\nu_{ei} \equiv \Lambda/(2 \ln\Lambda) \sim 16\text{--}19$, the cooperative motions of collisionless electrons are still essential in the electron dynamics.

Figure 3(b) shows, as a function of the velocity of the plasma from the left plane v (i) the mean free path (λ_{ii}), (ii) the timing (t_i) at which plasma leaving the left plane at $t = 0$ with velocity v intersects plasma from the right plane moving with trajectory $x = x_0 - V_s t$, (iii) the compression ratio (v_1/v_2), where the upstream plasma velocity $v_1 = v + V_s$ and $v_2 = V_s$. The right-hand axes show the normalized values $\lambda_{ii}\omega_{pi}/c$ and $t_i\omega_{pi}$, and the Mach number estimated using the brightness temperature M_B . In the experiment the plasma from the left plane is not all launched at $t = 0$; it can also be emitted at $t > 0$. Moreover, the plasma from the right plane can ablate the left plane to produce secondary plasma. Therefore, its actual velocity can be larger but not smaller than v ; the mean free paths and the compression ratio can hence be larger than our estimates. The mean free path is calculated

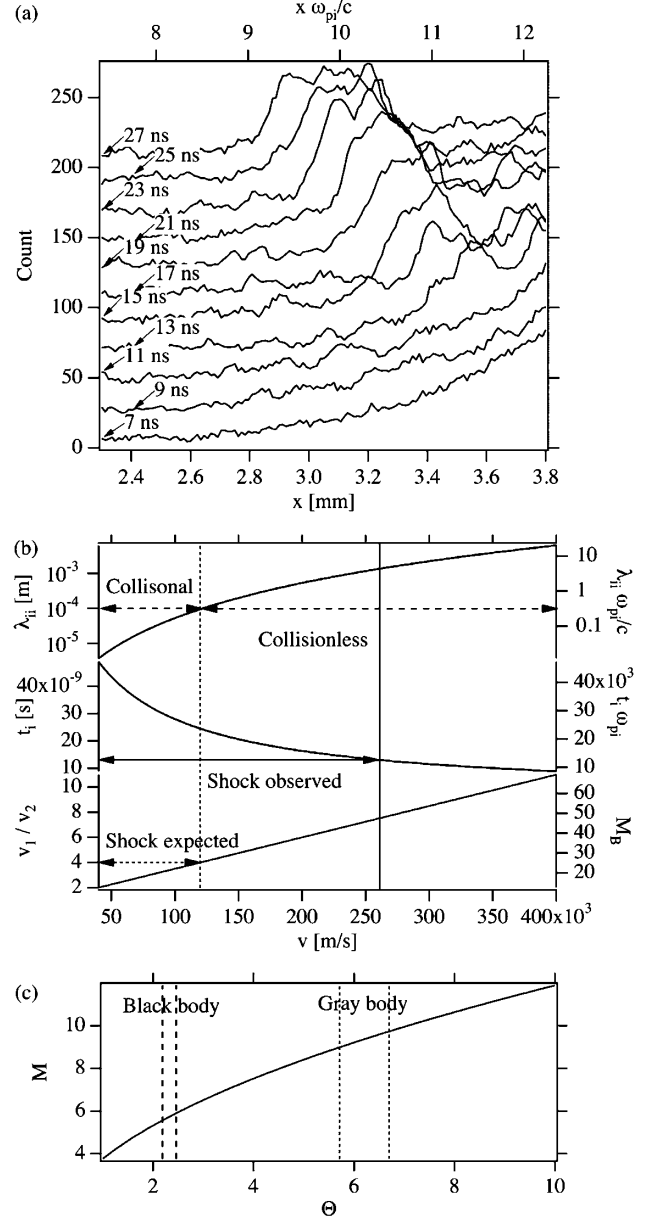


FIG. 3. (a) Stacked plot of line profiles of the SOP image in Fig. 2(b) from 7 to 27 ns. (b) Plotted against the velocity of the plasma from the left plane, from top to bottom: the mean free path of ions, the time at which plasma from the left plane reaches the shock, and the ratio of the upstream velocity ($v_1 = v + V_s$) to the downstream velocity ($v_2 = V_s$) are plotted against the plasma velocity from the left plane. (c) Mach number estimated from the observed temperature ratio of the left and right plasmas.

using the sum of the bulk-counterstreaming velocity and the ion thermal velocity in the downstream when $T_i = 21$ eV for the average relative velocity of collisions between upstream and downstream ions. At $v \sim 120$ km/s the mean free path is $\sim 100 \mu\text{m}$, indicated by the dashed arrow, and thus below this velocity the counterstreaming interactions are collisional and above this velocity they are collisionless. The solid arrow corresponds to $t = 13$ ns ($t\omega_{pi} = 1.3 \times 10^4$), the time when the shock started to

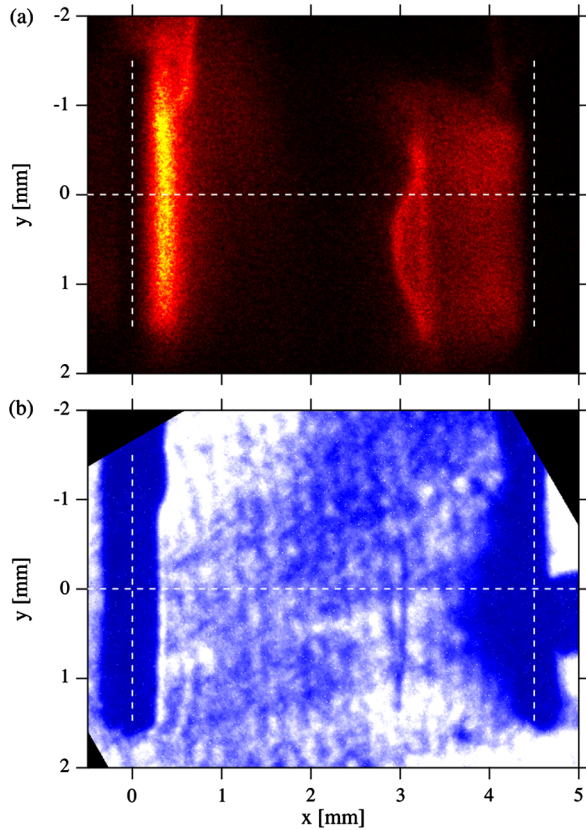


FIG. 4 (color online). (a) Self-emission snapshot at $t = 25$ ns taken on the same shot as Fig. 2. (b) Shadowgraphy snapshot at $t = 25$ ns taken on a different shot.

evolve; the observed shock structure is mostly in the collisionless regime. The transition from collisionless to collisional interactions seems smooth and we observed the shock structure following several tens of ns after this (not shown). The conventional theory predicts that the compression ratio $v_1/v_2 \equiv \rho_2/\rho_1 \rightarrow 4$ as the Mach number approaches infinity when $\gamma = 5/3$, indicated by the dotted arrow. We observed the compression ratio to be above this limit in the collisionless regime. The brightness Mach number M_B gives very large values, 25–47, which are overestimated since the brightness temperature is underestimated; the gray body assumption reduces the Mach number to 12–24.

The Mach number can also be estimated from the temperature difference as $M \approx 3(Y + 1)/Y(\pi\Theta/8)^{1/2}$, where Y and Θ are the density and temperature ratios between the two plasmas [5]. Since it is difficult to obtain a density map late in time, we set the Y to unity. The Mach number is plotted in Fig. 3(c). The dashed and dotted lines represent the observed temperature ranges under the black and gray body assumptions. Since the black body assumption underestimates the temperature difference, the Mach number at 5.6–5.9 is also underestimated. The gray body assumption yields $M \sim 9$ –9.7, which is rough but reasonable when compared with the Mach number estimation from the upstream flow velocity with the gray body assumption.

Figures 4(a) and 4(b) show self-emission GOI and shadowgraphy snapshots of the shock structures at $t = 25$ ns ($t\omega_{pi} = 2.4 \times 10^4$). The GOI image was taken on the same shot as the streak images in Fig. 2, but the shadowgraph was taken on a different shot. The vertical and horizontal dashed lines are the target positions and the nominal positions of the regions of the plasmas imaged onto the streak camera slits, respectively. In Fig. 4(a) a bow-shock-like structure is clearly seen in front of the right plane at $x \sim 3$ mm. The curvature of the shock fronts indicates that actual shock thicknesses can be thinner than those seen in SOP line profiles; broadening can take place in the projection of the self-emission onto the detection plane. In Fig. 4(b) a flat filament is seen at a similar position $x \sim 3$ mm (even though it was taken on a different shot), indicating the presence of a large density jump. There are ghost fringes all over the image, but the feature is genuine as it was not seen in the reference shot and similar structures were seen on two other shots at a similar timing (not shown).

These results strongly indicate the presence of electrostatic collisionless shock formation in very-high-Mach-number counterstreaming plasmas. Weibel filaments were not seen in our experiment; much larger laser energy is necessary to excite a Weibel-mediated shock [7]. In order to create such a shock, we are planning to perform a larger-scale experiment with the world's largest laser at the National Ignition Facility.

The authors would like to thank N. Ozaki, R. Yamazaki, M. Hoshino, T.N. Kato, S. Matsukiyo, T. Hada, and V. Krasnoselskikh for their helpful comments. A part of the calibration experiment was performed at the University of York under support of CIHEDS office.

*kuramitsu-y@ile.osaka-u.ac.jp

- [1] R. Z. Sagdeev, *Cooperative Phenomena and Shock Waves in Collisionless Plasmas*, in *Reviews of Plasma Physics*, edited by M. A. Leontovich (Consultants Bureau, New York, 1966), Vol. 4, p. 23.
- [2] R. J. Taylor, D. R. Baker, and H. Ikezi, *Phys. Rev. Lett.* **24**, 206 (1970).
- [3] H. Ikezi, T. Kamimura, M. Kako, and K. E. Lonngren, *Phys. Fluids* **16**, 2167 (1973).
- [4] H. Bailung, Y. Nakamura, and Y. Saitou, *Phys. Plasmas* **15**, 052311 (2008).
- [5] G. Sorasio, M. Marti, R. Fonseca, and L. O. Silva, *Phys. Rev. Lett.* **96**, 045005 (2006).
- [6] T. N. Kato and H. Takabe, *Astrophys. J. Lett.* **681**, L93 (2008).
- [7] H. Takabe *et al.*, *Plasma Phys. Controlled Fusion* **50**, 124057 (2008).
- [8] Y. Kuramitsu *et al.*, *Astrophys. J. Lett.* **707**, L137 (2009).
- [9] T. Morita *et al.*, *Astrophys. Space Sci.*, doi:10.1007/s10509-010-0525-5 (2010).
- [10] L. Spitzer, *Physics of Fully Ionized Gases* (Interscience, New York, 1962).